AerospaceEurope Conference2021
WARSAW, POLAND | 23 -26 NOVEMBER 2021
CEAS Council of European Aerospace Societies

DESIGN AND CFD ANALYSIS OF THE LOX/LCH4 DUAL REGENERATIVE COOLING CIRCUIT OF THE DEMOP1 DEMONSTRATOR

G. Esnault1[1], F. Rossi[2]

[1,2]Pangea Aerospace, Calle Roc Boronat, 117, 08018 Barcelona, Spain

Abstract

Aerospike engines have always been of interest because of their altitude adaptation properties leading to higher performances compared to equivalent classical bell nozzles. Regardless, because of their dimensions and configuration, aerospike engines experience a higher integral heat flux, especially at the throat. Cooling this type of engine becomes a real challenge. This is one of the main reasons for the lack of research and industrialization since the aerospike concept first appeared in the 50s. However, because of the recent development of novel manufacturing techniques, such as additive manufacturing, aerospike engines are experiencing a renewed interest. The flexibility of additive manufacturing allows the cooling channel circuit design to reach a new level of freedom. Moreover, the LOX/LCH4 regenerative cooling system is expected to affect positively the engine development improving reusability and reducing toxic substances in the plume.

This study documents the research, design, and Computational Fluid Dynamics (CFD) analysis of the regenerative cooling system for the DemoP1 demonstrator developed by Pangea Aerospace. DemoP1 is the first aerospike engine fully additively manufactured using copper alloys and including a dual regenerative cooling circuit. The CFD analysis has been performed with the commercial software ANSYS Fluent. Finally, the challenge of numerically simulating both the trans-critical coolant and the high roughness environment will be discussed.

Keywords: aerospike, cryogenic propulsion, additive manufacturing, dual regenerative cooling, LOX/LNG

1. Introduction

DemoP1 is the aerospike engine demonstrator developed by Pangea Aerospace since mid-2019, with a test campaign programmed in October 2021. Its main characteristics are reported in Table 1.

Table 1 - DemoP1 high-level specifications

Propellants	LOX/LNG
Cycle	Pressure-fed
Thrust (sea level)	20 kN
Specific impulse (sea level)	268 s
Mixture ratio	2.8
Expansion ratio	5
Dimensions	240 x 240 x 260 mm

DemoP1 is composed of two parts, the external and the internal, also referred to as plug, additively manufactured with copper alloys. The two parts can be observed in Figure 1.

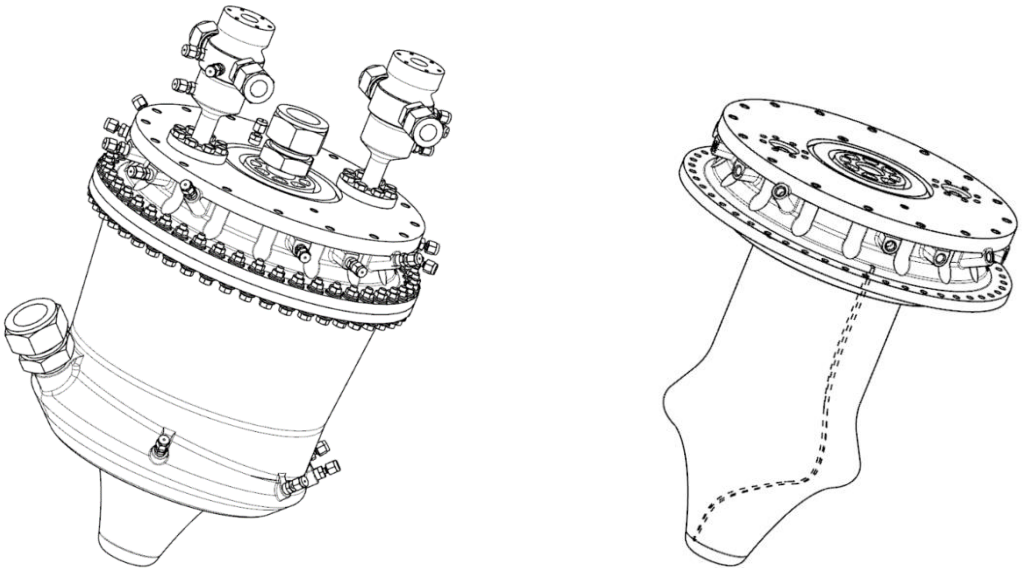

Figure 1 - DemoP1 solid model (left) - Plug with a LOX cooling channel trace (right)

Since the combustion chamber is made by the combination of these two components, the hot flow is in interaction with both the external and the internal parts. Therefore, it makes the thermal management of the aerospike challenging because of the resulting surface to be cooled. With the mass flow rate available for the regenerative circuit being fixed by the chosen thrust, a dual regenerative cooling system was designed with oxygen flowing in the internal cooling circuit and methane in the external one. Thus, this paper will present and discuss the strategy adopted by Pangea Aerospace to design and analyze the cooling circuit of the DemoP1 demonstrator.

2. Design

One of the first step of the pre-design of the aerospike engine was the development of an inhouse MATLAB tool to design and predict the cooling performances of the designed channels for both the external and the plug of the aerospike. It is a first order analysis based on semi-empirical relations. From the engine geometry, the combustion chamber hot flow properties and the channel geometrical inputs chosen, the code discretizes the geometry in order to solve the heat transfer taking place at the engine liner. It is a 1D tool, which also means that only the radial direction is considered and consequently the longitudinal and circumferential direction are neglected. The constraints set by additive manufacturing have to be taken into account in the implementation of the geometry. In fact, the minimum dimensions of the channels are fixed at 1mm because of the printer tolerances. Therefore, the printing angle of the engine leads to different roughness profiles along the channels, whose influence on the heat transfer calculation cannot be neglected. Modelling the heat transfer coefficient on the coolant side of both trans-critical oxygen and methane has proved to be delicate. Several correlations are available in the literature but were not developed for additively manufactured cooling channels.

The objective of the heat transfer function of the tool is to solve the thermal equilibrium in order to calculate the liner temperature. This thermal equilibrium is a sum of several thermal phenomena: the convection on the hot gas side, the conduction through the material and the convection on the coolant side.

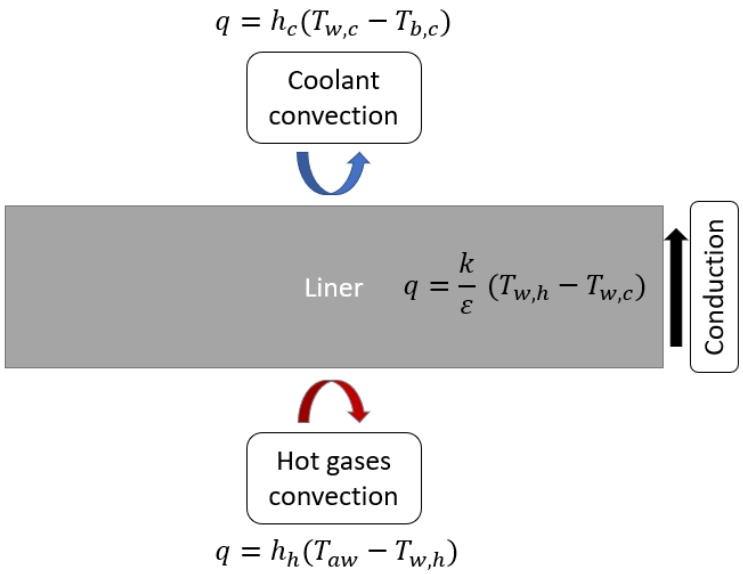

Figure 2 - Thermal Phenomena

Therefore, the heat flux can be expressed with this equation:

$$q = \frac{T_{aw} - T_c}{\frac{1}{h_h} + \frac{\varepsilon}{k} + \frac{1}{h_c}} = h_h(T_{aw} - T_{liner}) \quad (1)$$

Moreover, experiments were conducted to determine the density, the specific heat and the thermal conductivity of the copper alloy used to print the engine. These data were implemented as inputs in the MATLAB tool and the CFD setup which will be described further.

2.1 Hot gas side heat transfer

The chamber and the nozzle geometries are the result of another MATLAB code developed inhouse that will not be discussed in this paper. The hot flow properties were therefore provided by this other tool using CANTERA [1]. To assess the heat transfer convection problem on the hot gas side, the Nusselt number correlation developed by D.R. Bartz [2] was used:

$$htc_h = \frac{0.026}{D_t^{0.2}} \frac{\mu_0^{0.2} c_{p,0}}{Pr_0^{0.6}} \left(\frac{p_0}{c^*}\right)\left(\frac{At}{A}\right)^{0.9} s \quad (2)$$

$$s = \left[\frac{1}{2}\frac{T_{u,wh}}{T_0}\left(1 + \frac{\gamma - 1}{2}M^2\right) + \frac{1}{2}\right]^{-0.68} \left[1 + \frac{\gamma - 1}{2}M^2\right]^{-0.12} \quad (3)$$

However, it has already been demonstrated [3] that for an oxygen/methane engine, the heat flux was overpredicted (cf Figure 4).

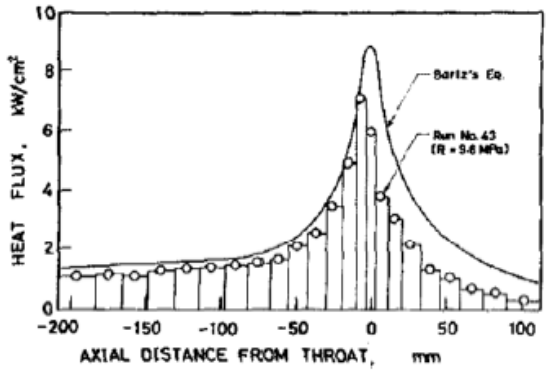

Figure 3 - Comparison of experimental heat flux with prediction from Bartz correlation for oxygen/methane engine

A CFD analysis, whose numerical setup will be discussed later, was performed in order to determine the amount of overprediction we were experimenting in our case.

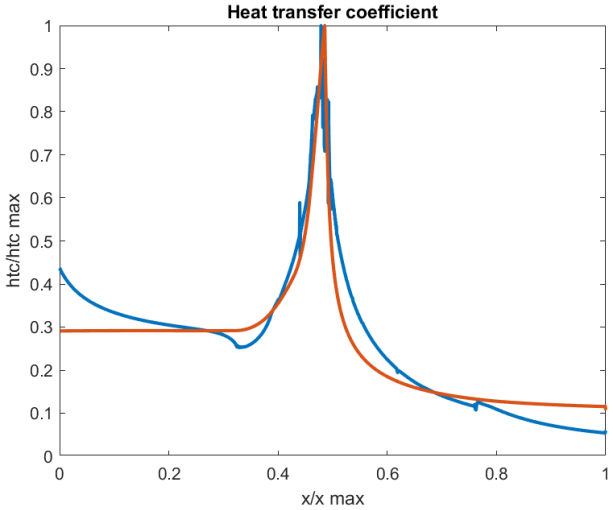

Figure 4 - Heat Transfer Coefficient ((a): corrected MATLAB, (b): fluent)

The correction factor added to the 1D tool is in the order of 25% of overprediction of the maximum heat flux, similar to the factor discussed in [3].

It should also be noted that radiation was not considered in the 1D tool, neither in the CFD simulation, since the largest contribution to the heat flux from the hot gases is due to convection.

2.2 Heat transfer coolant side

In addition to the hot-gas side of the liner, the heat transfer has to be characterized on the coolant side.

The cooling channels on the plug will be first addressed since they represent the main critical element: the high heat flux area being larger on the plug than on the external. The plug is cooled by flowing propellant from the nozzle tip to the injector plate in order to get the best coolant properties at the throat region, where the peak of the heat flux is experienced. With the propellant mass flow rates being imposed by the chosen thrust of the engine, the logical choice is to feed the plug cooling channels with LOX. The mixture ratio of the engine is 2.8, as illustrated Table1, thus there is more oxygen available for cooling the more challenging plug. Using oxygen in the cooling circuit is not trivial. In case some cracks develop in the oxygen circuit side, this could lead to a catastrophic failure [4]. However, according to [5], for temperatures below 900K copper alloys are not susceptible to combustion with liquid oxygen.

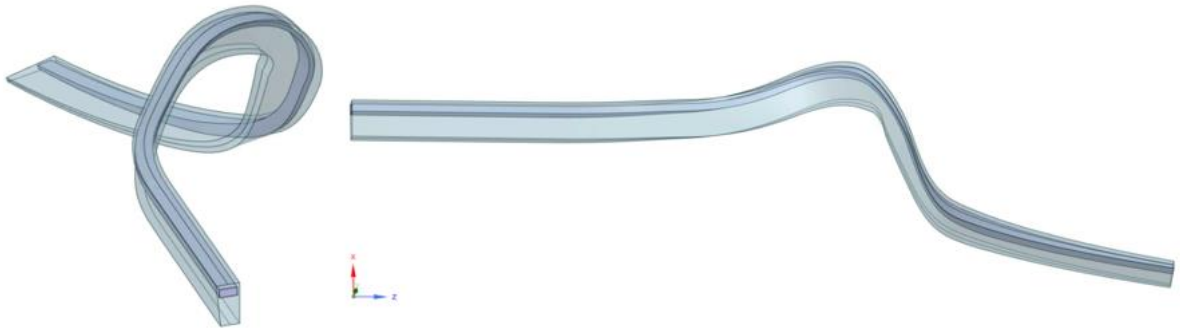

Figure 5 - LOX plug cooling channel

The spiral shape of the cooling channels of the engine plug can be observed in Figure 6. This design strategy has been adopted to cope with the increasing diameter at the plug throat while still being able to maintain the cooling efficiency by keeping a cooling channel aspect ratio ≥ 1.

The choice of the correlation to model the heat transfer on the coolant side has been challenging. In fact, the particularity of the manufacturing process and the lack of such considerations on the classical formulations of the Nusselt correlations in the literature had to be faced.

The decision has been made to use the Nusselt correlation for supercritical oxygen developed by NASA [6], for the pre-design step, while tuning it according to CFD results and other sources that will be presented later:

$$Nu_b = 0.0025 Re_b Pr_b^{0.4} \left(\frac{\rho_b}{\rho_w}\right)^{-\frac{1}{2}} \left(\frac{k_b}{k_w}\right)^{\frac{1}{2}} \times \left(\frac{Cp_{ia}}{Cp_b}\right)^{2/3} \left(\frac{P}{Pcr}\right)^{-1/5} \left(1 + \frac{2}{L/D}\right) \quad (4)$$

After the plug, the external cooling circuit has been dimensioned and analysed. It also presented a challenge from a cooling standpoint considering the modest methane mass flow rate available together with the high surface to be cooled. The solution adopted for DemoP1 was a combination of up-cooling and down-cooling. The idea is to first flow liquid methane from the injector plate to the throat in order for the coolant to get enough heat to become trans-critical and thus improve its cooling efficiency at the throat. Then, the coolant has to flow up again, which will improve even more the cooling at the throat by the implementation of a U-turn at the bottom of the external, to finally reach the injector plate manifold.

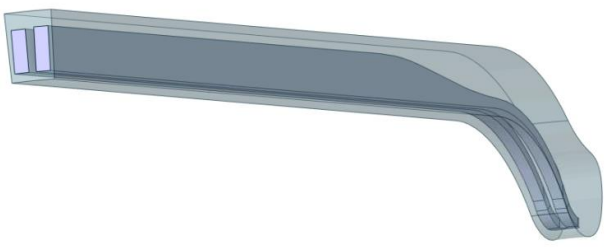

Figure 6 - LCH4 external cooling channel

To model the heat transfer on the methane side, the correlation developed by Pizzarelli [7] was employed. The decision was made to add margins to the results obtained with this correlation since the heat transfer deterioration phenomenon associated to trans-critical coolant will be partly compensated by the high roughness height of the additively manufactured cooling channels.

$$Nu = 0.0026 Re_b^{0.8} Pr_b^{0.16} \Delta^{0.28} \tag{5}$$

With $\Delta = \frac{\rho_w}{\rho_b}\frac{k_w}{k_b}\frac{\overline{c_p}}{c_{p,b}}\left(\frac{\mu_b}{\mu_w}\frac{T_b}{T_w}\right)^2$

Finally, for both the internal and the external part of the aerospike, a correction factor in the coolant side heat transfer coefficient was added to take into account the channel roughness.

$$h_c = \frac{k(Nu\varphi_\xi)}{D} \tag{6}$$

$$\varphi_\xi = \frac{1 + 1.5 Pr^{-\frac{1}{6}} Re^{-\frac{1}{8}} (Pr - 1)}{1 + 1.5 Pr^{-\frac{1}{6}} Re^{-\frac{1}{8}} (Pr\xi - 1)} \xi \tag{7}$$

$$\xi = \frac{f_D(Re, hs)}{f_D(Re, hs = 0)} \tag{8}$$

3. Computational model

3.1 CHT iterative procedure

To solve the conjugate heat transfer taking place at the wall of the engine with CFD, it was decided to adopt a similar iterative procedure as the one described in [8]. Consequently, the problem was divided in subproblems that are then coupled by imposing specific boundary conditions. On one hand, the hot gas flow through the chamber and the nozzle simulation to assess the problem of convection taking place in the hot gas side of the liner. On the other hand, the cooling channel with the solid and fluid domains to solve the conduction through the solid and the convection on the coolant side.

In the first place, in order to get the adiabatic wall temperature on the hot gas side, a simulation of the nozzle geometry with the hot gas flow is performed considering adiabatic walls.
Secondly, to start the iterative procedure, the hot gas side is solved applying a temperature profile at the wall. The first guess of the liner temperature is taken from the result of the MATLAB 1D analysis. Then, a conjugate heat transfer analysis with the solid and the fluid domains of the cooling channel is conducted. On this last CFD case, the heat transfer coefficient calculated from the heat flux data of the hot gas simulation is applied, together with the adiabatic wall temperature as boundary condition to the liner:

$$h_c = \frac{q_{w,hg}}{T_{aw} - T_{w,hg}} \tag{9}$$

Once the case is converged, the wall temperature on the liner of the cooling channel case can be extracted. This new temperature can be applied to the hot flow simulation and the previous steps should be repeated until reaching convergence of the results for the liner temperature.

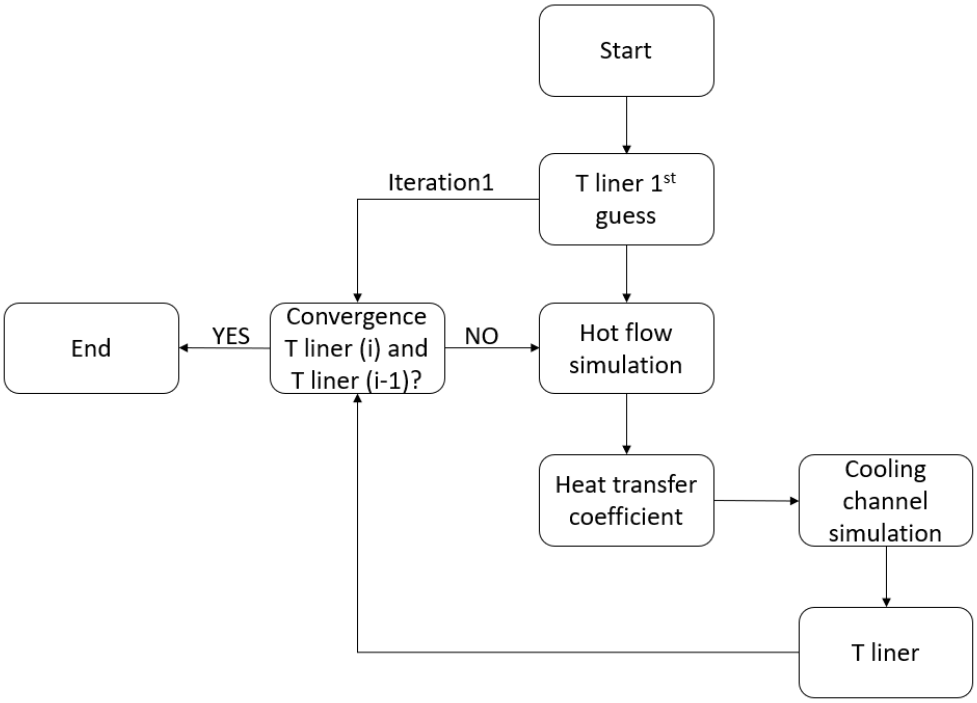

Figure 7 - CHT iterative procedure

3.2 Hot gas flow simulation

For the hot gas flow simulation, a 2D axisymmetric nozzle geometry discretized with a structured mesh of 886 000 cells was considered, which was refined at the wall in order to guarantee a y+≈1. This mesh was validated after having conducted a mesh dependency study.

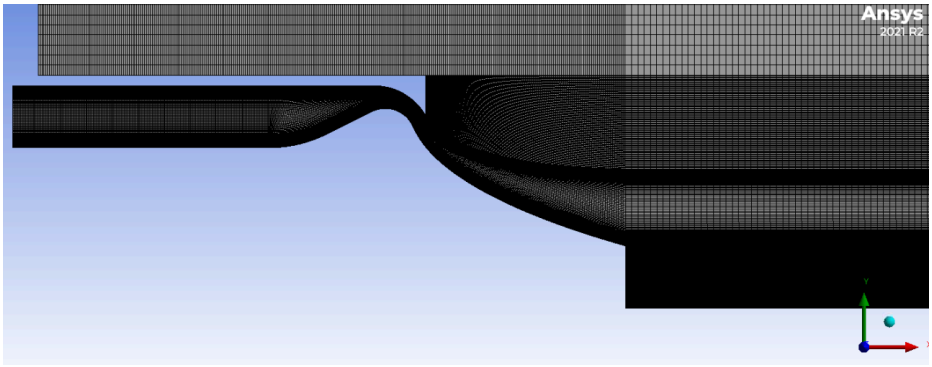

Figure 8 - 2D axisymmetric structured mesh

For the hot gas side simulation, it was assumed that combustion is already fully completed at the inlet and the flow is considered as a non-reactive mixture of the five main products of the oxygen and methane combustion: CO, CO2, H2, H2O and OH. RPA was used, with the engine parameters, to determine the mass fraction of each component.
The boundary conditions were as described in the previous paragraph:

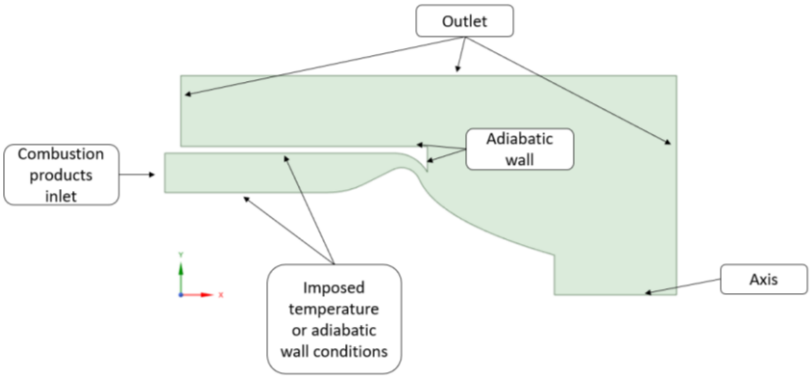

Figure 9 - Hot gas simulation boundary conditions

To model the density of this mixture, the real gas Redlich-Kwong model was used. For the transport properties, it was decided to use temperature-dependent user-defined functions (UDFs). These relations were calculated using CANTERA. To model the turbulence, the k-ω SST model was implemented because of its capacity to solve with high accuracy the near wall and the far wall zones. Convergence criteria of 10-3 and 10-6 for the residuals of continuity and energy respectively were assumed, as well as physical quantities stability. Several data, such as Mach number and pressure, were confronted against RPA results in order to validate the model used:

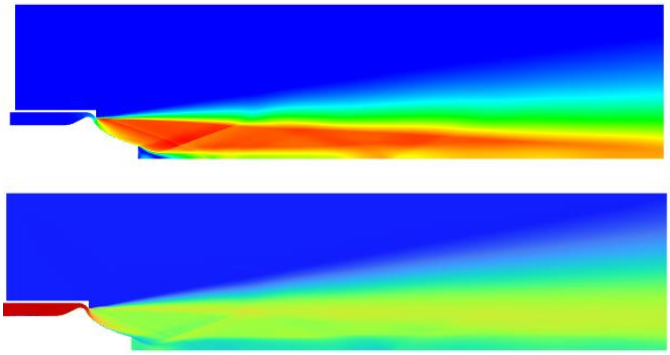

Figure 10 – Mach number contour (top) - Pressure contour (bottom)

The results of those simulations were, in particular, the heat transfer coefficient at the walls used as boundary condition to the CHT analysis.

3.3 Cooling channel simulation

For the cooling channel, a steady-state solution and a pressure-based method were chosen to solve the governing equations of continuity, momentum and energy. The roughness variation of the channel internal walls was considered by implementing a profile with UDFs. UDFs were also used for the heat transfer coefficient and adiabatic wall temperature profiles coming from the hot gas side simulation. After comparing several turbulence models, a topic that will not be developed in this paper, the k- ω SST turbulence model was finally adopted because of its wall distance automatic behaviour and its accuracy in solving heat transfer problems, as discussed in [9]. A coupled scheme was chosen to couple pressure and velocity and a second order spatial discretization was used. The supercritical fluid is described using the NIST real gas model for best description of the sharp property variation around the trans-critical point. Convergence criteria of 10-3 and 10-6 for the residuals of continuity and energy were assumed, respectively, as well as physical quantities stability. To model the conduction trough the solid, the Fourier's equation is solved. To take into account the evolution of material properties with temperature, UDFs were created based on the measures made on samples printed with the same printer and same alloy as the engine.
The particularity of the additively manufactured cooling channels, related to the roughness of the printed specimen, makes the mesh of the near-wall area questionable. In order to assess the problem and get a better idea of what could be done, several mesh densities were simulated. The results from the different configurations were not conclusive. In fact, the mesh dependency study led

to the conclusion that the 1st cell size has a noticeable impact on the heat transfer calculation. This point will be discussed further in this article.

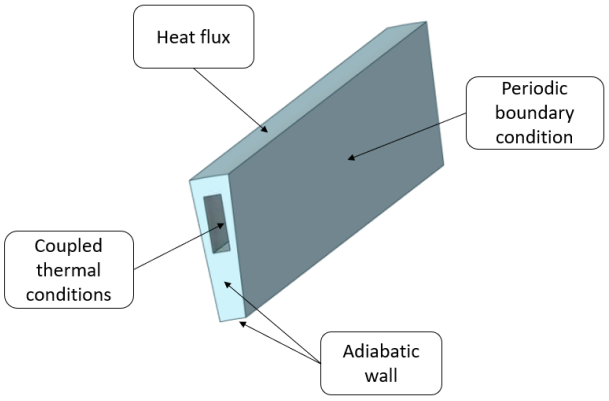

Figure 11 - Cooling channel simulation boundary conditions

Finally, the liner temperature profile convergence was reached after 2 or 3 iterations between the hot gas simulation and the cooling channel simulation.

4. Results and discussion

The results of the hot gas side CFD analysis are reported on the upper left of the Figure 14 for the internal contour and on the upper left of the Figure 15 for the external contour. Validation was ensured comparing the core flow properties with RPA data, as mentioned in the previous part.

Regarding the cooling channel analysis, the final results for the oxygen side simulation are illustrated in Figure 14:

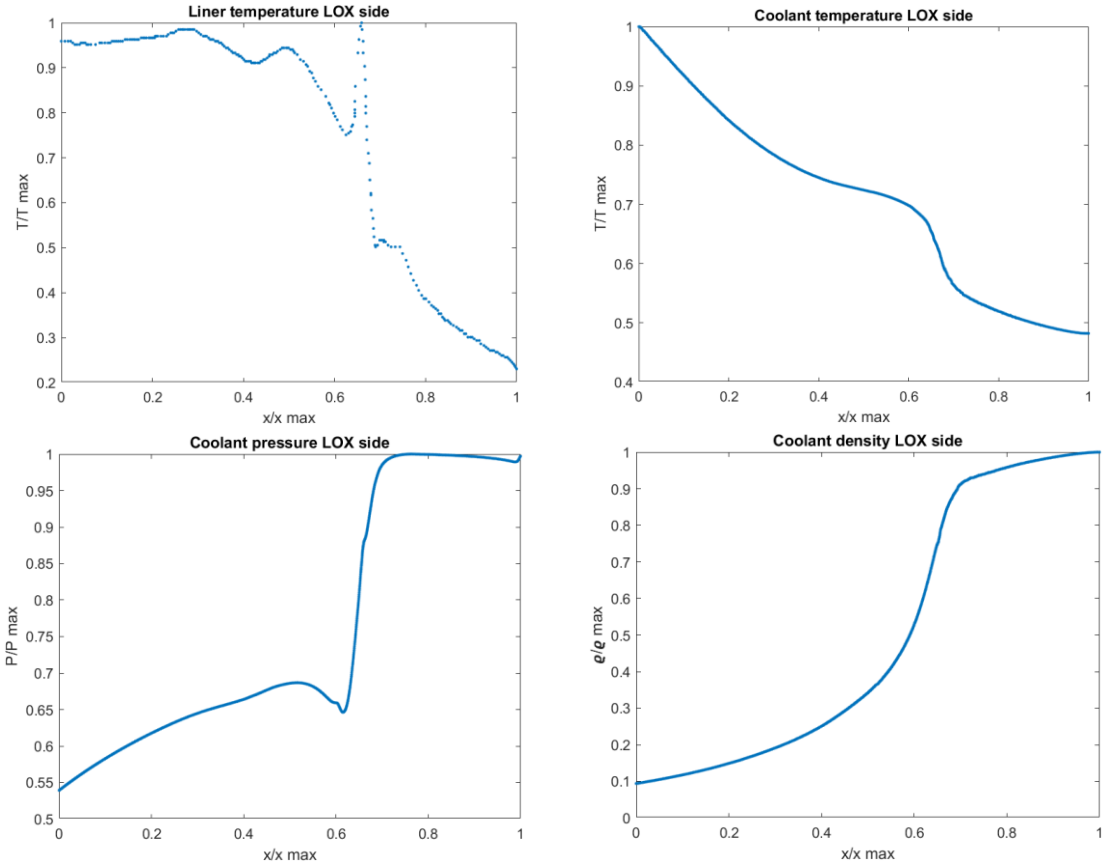

Figure 12 - LOX cooling channel CFD results

The behavior of the coolant temperature, pressure drop and density can be observed as a function of the engine axis from the injector plate (x/xmax=0).

The results for the methane cooling channels are illustrated in Figure 15:

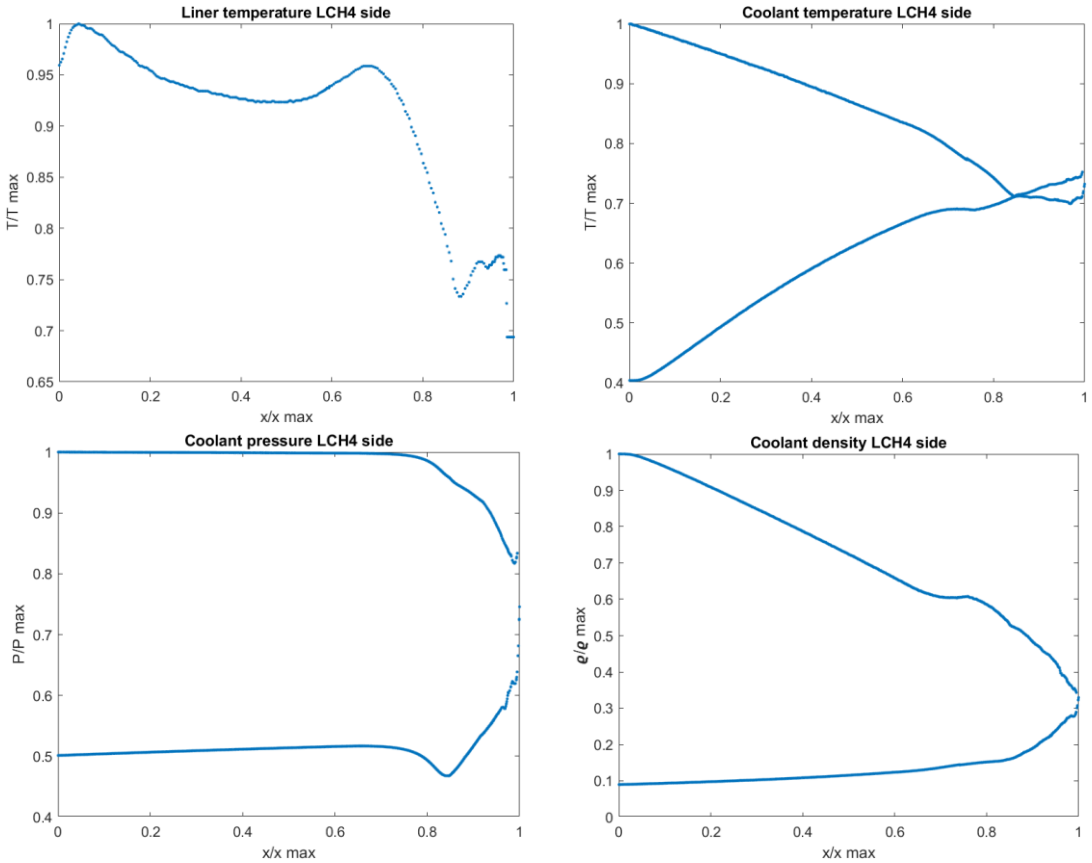

Figure 13 - LCH4 cooling channel CFD results

In Figure 15, the coolant is characterized on its path, that is composed of two opposite directions. First the coolant flows from the injector plate to the throat of the engine and then, in the opposite direction, to the injector plate. This solution was adopted to cope with the high temperature experienced at the throat.

Regardless, as mentioned on the precedent paragraph, the mesh refinement level has shown to have an important impact on the heat transfer evaluation on the cooling channel side and the strategy adopted to get these results will be now discussed. To illustrate this point, the cooling channel on the internal part is taken as an example. This is the one requiring more work because of its particularly atypical roughness profile (cf. Figure 16).

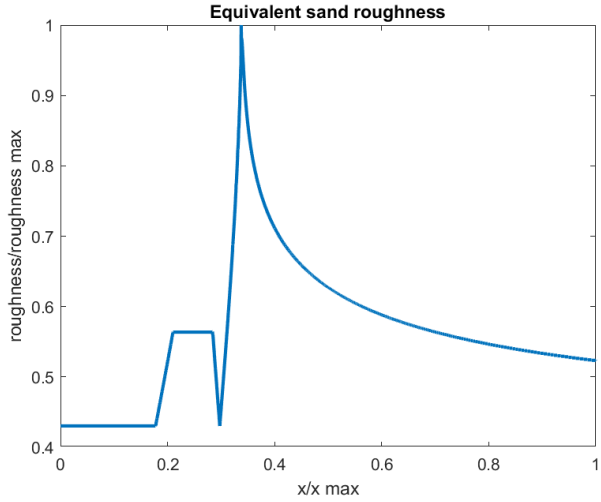

Figure 14 - Roughness profile on the LOX cooling channel

Several mesh refinements of the cooling channel geometry were computed and are reported in Figure 17:

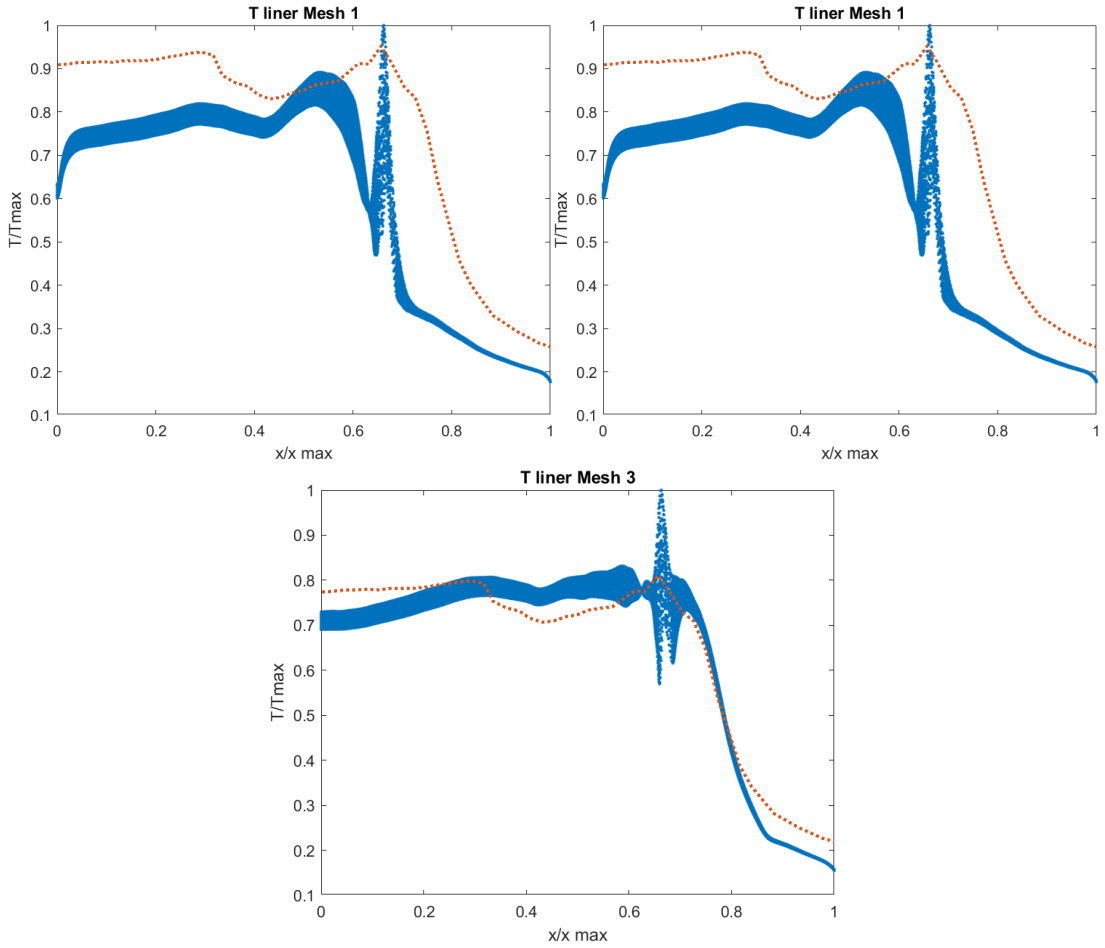

Figure 15 - Liner temperature obtained with different mesh refinements ((a): Reference temperature profile (b): Liner temperature obtained with CFD)

From Figure 17, an important variation of the liner temperature profile can be noticed, depending on the level of refinement on the boundary layer. Once starting this simulation activity, the problem on how much the boundary layer should be discretized was central. Indeed, on the commercial software Ansys Fluent, several models are proposed to simulate the roughness according to its height. Usually, a good practice is to respect the rule: the 1st cell height should be at least twice the size of

the roughness height [10]. After physically measuring the roughness height on samples, the calculation of the equivalent sand-grain roughness, K_s, was performed using the correlation presented in [11]. The K_s^+ factor was then computed and the characterization of the cooling channel as fully rough was made:

$$K_s^+ = \rho \,.\, \mathrm{K_s} \,.\, \sqrt{\frac{\tau}{\rho}\frac{1}{\mu}} \tag{10}$$

As a matter of fact, in Ansys Fluent, the fully rough regime is considered for K_s^+ greater than 90. In Ansys Fluent, this is equivalent to creating a virtual shifting of the wall using the function ΔB :

$$\Delta B = \frac{1}{\kappa}\ln(1 + C_s K_s^+) \tag{11}$$

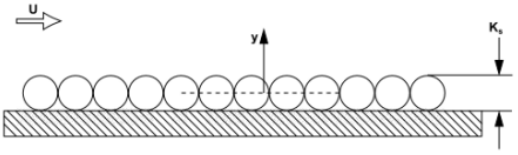

Figure 16 - Illustration of the Equivalent Sand-Grain Roughness [10]

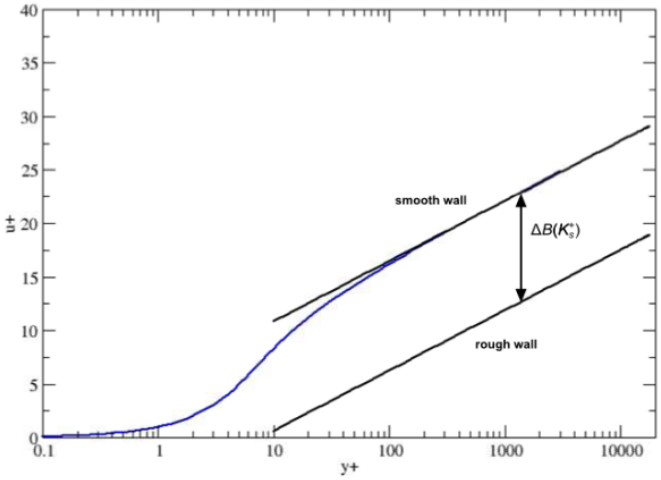

Figure 17 - Downward Shift of the Logarithmic Velocity Profile [10]

As can be seen from the expression of ΔB , the shift of the logarithmic profile is dependent not only on K_s^+ but also C_s, which is known as the roughness constant. Cs is a value going from 0.5, that represents a homogeneous repartition of the sand grains, to 1, for a representation of an irregular repartition of the sand grains. Because of the lack of experimental data, the calculation was based on a model using a Cs=0.5. This approach leads to a dependence relation between K_s^+ and y^+ :

$$K_s^+ = \min(K_s^+, y^+) \tag{12}$$

In other words, reducing y^+ to a smaller value than K_s^+ will consist in cutting the roughness height implemented. This has been directly observed with the different cases run on the cooling channel, as showed in Figure 20.

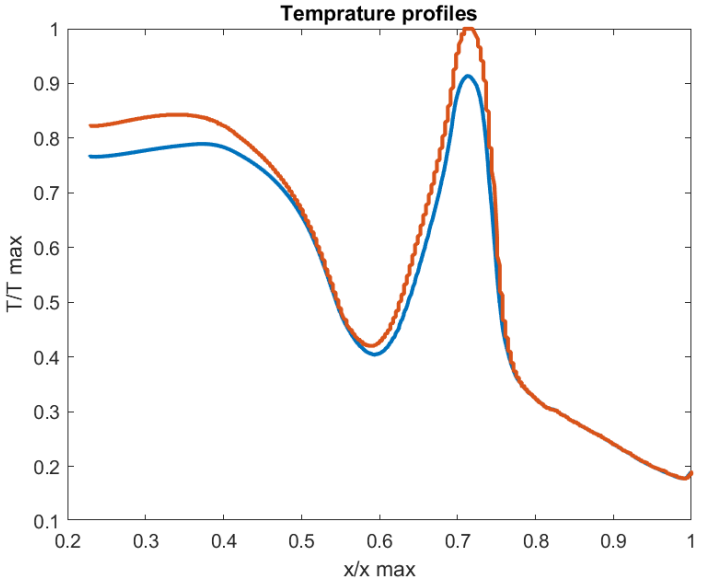

Figure 18 - Temperature obtained with different 1st cell size ((a): y=2.2e-6m (b): 4.8e-6m)

In this example, the 1st cell wall distance for the red line case was about half of the one used for the blue line case. It can be observed that, in some areas, the temperature profile is shifted. According to the above-mentioned definition of the fully rough regime management by Fluent, it would be the equivalent as cutting the roughness height.

However, applying the 1st cell size adapted to the roughness height, with additively manufactured cooling channels, would make the mesh too coarse to properly solve the heat transfer taking place near the wall. As a matter of fact, strong gradients are observed on the near wall region such as the density variation along the radial axis of the engine when the propellant gets trans-critical. Consequently, not discretizing the linear part of the boundary layer would potentially induce an error on the evaluation of the heat transfer coefficient. Thus, the size of the first cell needs to be a trade-off between the roughness effect and the capture of the near-wall compressibility. Since these two parameters are irregularly changing along the cooling channel, the simulated geometry has to be divided in several pieces, 10 in this case, in order to independently refine the mesh of the different subsections.

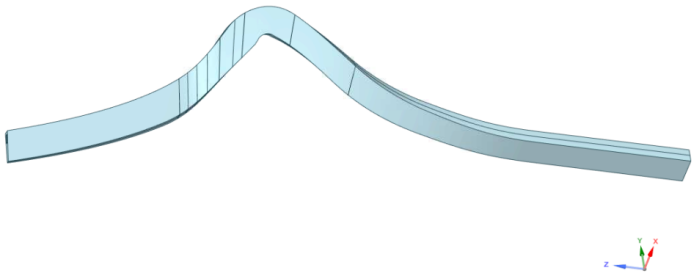

Figure 19 - Sliced LOX cooling channel geometry

Regarding the evaluation of the size that should be applied on the 1st cell of each subsection, this is the result of an iterative process. It was observed that a too refined mesh is leading to an overprediction of the liner temperature and, in opposition, a too coarse mesh at the boundary layer is underestimating the temperature. The iterative method applied to the mesh was possible considering the results of a proprietary code considered as reference (curve (a) Figure 17). This tool was designed with a modified Frolov [12] heat transfer correlation according to tests performed on additively manufactured cooling circuits. This correlation was developed and verified for supercritical

oxygen and methane. This method, while representing the closest accuracy possible at the time it was used, is not ideal and future activities are already ongoing at Pangea Aerospace to improve the adopted heat transfer correlation. For this purpose, a characterization of cooling channels printed at different angles (leading to a different roughness height) and cooled by the two propellants is planned. Another solution would be to concentrate the efforts on the numerical model simulating the physical roughness profile with different flow properties in order to define a new correlation and determine a modified momentum equation with added source and sink terms to represent the impact of such roughness profiles. This last solution is ongoing in partnership with different European universities and research centers. Finally, an option on the manufacturing side is also being evaluated. In fact, the application of a state-of-the-art internal polishing process would allow to control and uniform the roughness inside the channels. Consequently, the problems to face would be closer to cases already studied, such as the one found in [13].

5. Conclusion

DemoP1 is a LOX/LCH4 aerospike engine demonstrator that will be tested during the last semester of 2021. The design and development have been supported by extensive FEA and CFD studies and the results of this test campaign will lead the development of the second engine developed by Pangea Aerospace. Moreover, to continue to push the technological limits, several other activities have already been planned, in particular to cope with the limits encountered with CFD, highlighted across this article.

6. Contact Author Email Address

Email: contact@pangeaaerospace.com

7. Copyright Statement

References

[1] Cantera Matlab, https://cantera.org/

[2] D.R. Bartz, A simple equation for rapid estimation of rocket nozzle convective heat transfer coefficient, Jet Propulsion 27(1), pp. 49–51 (1957).

[3] H. Tamura, F. Ono, A. Kumakawa, and N. Yatsuyanagi, LOX/Methane staged combustion rocket combustor investigation, AIAA/SAE/ASME/ASEE 23rd Joint Propulsion Conference (San Diego, 1987), AIAA-87-1856, doi:10.2514/6.1987-1856.

[4] E. Armstrong; J. Schlumberger, Cooling of rocket thrust chambers with liquid oxygen, AIAA/SAE/ASME/ASEE 26th Joint Propulsion Conference (Orlando,FL,U.S.A. 16 July 1990 - 18 July 1990).

[5] I. N. Nikischenko, et al., Improving the performance of LOX/kerosene upper stage rocket engines, Propulsion and Power Research (2017), https://doi.org/10.1016/j.jppr.2017.07.008

[6] H.G.Price, Cooling of high-pressure rocket thrust chambers with liquid oxygen, NASA Lewis Research Center, Cleveland, Ohio, AIAA 80-1260R, Vol. 18, No.4, 2014

[7] Marco Pizzarelli, A CFD-derived correlation for methane heat transfer deterioration, Numerical Heat Transfer, Part A: Applications, 69:3, 242-264 (2016).

[8] M. Pizzarelli, B. Betti, F. Francesco, D. Ricci, P. Roncioni, F. Battista, V. Salvatore, Cooling channel analysis of LOX/LCH4 rocket engine demonstrator, Propulsion and Energy Forum, July 28-30, 2014, Cleveland, OH

[9] D.V. Brezgin, K.E. Aronson, F. Mazzelli, A. Milazzo, The surface roughness effect on the performance of supersonic ejectors, Thermophysics and aeromechanics, 24(4), 553-561, 2017

[10]Ansys Fluent User's Guide, 7.4.15 Wall Boundary Conditions

[11]T. Adams, C. Grant, H. Watson, A simple algorithm to relate measured surface roughness to equivalent sand-grain roughness, Avestia Publiching, International Journal of Mechanical and mechatronics, Volume 1, Issue1, Year 2012.

[12] Aspects of the non-film oxygen cooled LPRE chamber state analysis / Strizhenko P.P. / Bulletin of the Samara State Aerospace University / No.3 (19), 2009, pp. 191-196.

[13] Pizzarelli et al., High aspect ratio cooling channel flows, 49th AIAA joint propulsion conference, San Jose, AIAA 2013- 3998.